0026-895X/95/050956-09$3.00/0

MOLECULAR PHARMACOLOGY, 47:956–964 (1995).

Photoaffinity-Labeled Ligand Binding Domains on Dopamine Transporters Identified by Peptide Mapping

ROXANNE A. VAUGHAN

Neuroscience Branch, National Institute on Drug Abuse Addiction Research Center, Baltimore, Maryland 21224

Received October 28, 1994; Accepted March 1, 1995

SUMMARY

Binding domains on rat dopamine transporters for cocaine and 1-(2-diphenylmethoxy)ethyl-4-(3-phenylpropyl)piperazine compounds were identified using controlled proteolysis of photoaffinity-labeled protein and epitope-specific immunoprecipitation of the labeled fragments. Rat dopamine transporters were photoaffinity labeled with 1-[2-(diphenylmethoxy)ethyl]-4-[2-(4-azido-3-[^{125}I]iodophenyl)ethyl]piperazine ([^{125}I]DEEP) [a 1-(2-diphenylmethoxy)ethyl-4-(3-phenylpropyl)piperazine analog] or 3β-(*p*-chlorophenyl)tropane-2β-carboxylic acid, 4′-azido-3′-[^{125}I]iodophenylethyl ester ([^{125}I]RTI 82) (a cocaine analog) and were gel purified to remove contaminating radioactivity. The resulting samples were treated with V8 protease or trypsin and analyzed by sodium dodecyl sulfate-polyacrylamide gel electrophoresis. The peptide maps generated with each enzyme were different for each of the ligands, suggesting that the ligands were incorporated into different regions of the protein. Identical peptide maps were generated from striatum- and nucleus accumbens-derived transporters, indicating that these polypeptides are highly similar in primary sequence. The proteolytic fragments generated by V8 protease were localized to specific domains of the protein using antipeptide antibodies corresponding to five different regions of the transporter. Fragments of 10 and 7 kDa from [^{125}I]DEEP-labeled transporters were specifically immunoprecipitated with an antibody generated against amino acids 42–59 (near the first putative transmembrane domain), whereas a 34-kDa fragment from [^{125}I]RTI 82-labeled transporters was precipitated with three different sera corresponding to regions in the carboxyl-terminal two thirds of the protein. None of the V8 fragments smaller than 45 kDa, containing either photolabel, was altered in molecular mass by *N*-deglycosylation. The results indicate that photoincorporation of [^{125}I]DEEP occurs in the amino half of the dopamine transporter, near the first two transmembrane helices, whereas [^{125}I]RTI 82 labels the carboxyl-terminal region of the protein, between transmembrane domains 4 and 12.

Dopaminergic nerve transmission is regulated in part by the action of DATs, which couple the energy of electrochemical sodium gradients to DA uptake into presynaptic neurons (reviewed in Ref. 1). cDNAs for DATs have been cloned from human (2, 3), rat (4, 5), and bovine (6) brain. The deduced amino acid sequences predict proteins of 619 or 620 amino acids, with 12 putative TMDs and three or four consensus *N*-glycosylation sites. The current model for topology, based on the presence of consensus phosphorylation and *N*-glycosylation sites, places the amino and carboxyl termini intracellularly and the large loop containing the consensus glycosylation sites between TMDs 3 and 4 (2–6).

DA uptake is inhibited with a distinct pharmacological profile by a variety of structurally diverse compounds, including cocaine, mazindol, *N*-[1-[2-benzo(*b*)thiophenyl]cyclohexyl]piperidine, and GBR compounds, and radiolabeled analogs of these molecules have been used extensively to characterize DATs in binding assays (reviewed in Refs. 7 and 8). These compounds are also competitors in binding assays, with rank orders of potencies comparable to those for uptake inhibition. The molecular mechanisms by which these compounds compete against each other and inhibit uptake is not known. The experimental evidence describing the interactions of uptake blockers at the DAT is complex, with some data indicating that the compounds act competitively at a single site (9, 10) and other data suggesting noncompetitive actions at different sites (11–14). Determining the nature of the binding sites for these drugs is a primary step necessary to obtain insight into the molecular mechanism of DAT action and also is important for the possible development of therapeutic cocaine-blocking medications (15).

In addition to studies using reversible ligands, DATs have been studied with photoaffinity ligands representing two of the aforementioned classes of compounds. These compounds

This work was supported by the Intramural Research Program of the National Institute on Drug Abuse.

ABBREVIATIONS: DAT, dopamine transporter; [^{125}I]DEEP, 1-[2-(diphenylmethoxy)ethyl]-4-[2-(4-azido-3-[^{125}I]iodophenyl)ethyl]piperazine; GBR, 1-(2-diphenylmethoxy)ethyl-4-(3-phenylpropyl)piperazine; [^{125}I]RTI 82, 3β-(*p*-chlorophenyl)tropane-2β-carboxylic acid, 4′-azido-3′-[^{125}I]iodophenylethyl ester; TMD, transmembrane domain; WGA, wheat germ agglutinin; DA, dopamine; SDS, sodium dodecyl sulfate; PAGE, polyacrylamide gel electrophoresis.

are [^{125}I]DEEP, a GBR analog (16, 17), and [^{125}I]RTI 82, a cocaine analog (18). The structures of these compounds are shown in Fig. 1. These ligands label a glycoprotein of approximately 80 kDa, with appropriate pharmacological specificity, in membranes prepared from striatum, nucleus accumbens, and olfactory tubercle of rats, dogs, and humans, as well as a 100-kDa protein in COS-7 cells transfected with the DAT cDNA (19). Antibodies raised against several discrete amino acid sequences of the deduced DAT sequence immunoprecipitate both [^{125}I]DEEP- and [^{125}I]RTI 82-labeled proteins, demonstrating that the two ligands are incorporated into the same polypeptide (20).

In this study, the binding domains on striatal DATs for these two photoaffinity ligands were analyzed by peptide mapping, enzymatic deglycosylation, and epitope-specific immunoprecipitation. It was found that DATs labeled with the different ligands produced different proteolytic patterns, and immunological analysis of the peptide fragments localized the incorporation of the two ligands to different regions of the DAT polypeptide. This may support the contention that these ligands interact noncompetitively and provides information complementary to that obtained by molecular studies relating to the mechanism of DAT function.

The peptide-mapping procedure was also used to analyze the polypeptide structure of DATs obtained from the nucleus accumbens, a region whose dopaminergic terminals project from different cell groups, compared with striatal neurons (21). Ascertaining the biochemical characteristics of DATs from this region is of interest because the addictive properties of cocaine are more closely associated with actions in the nucleus accumbens than in the striatum (22); although binding and uptake activities of these transporters are essentially indistinguishable, other biochemical parameters appear to be different. For example, DATs from the nucleus accumbens but not the striatum undergo down-regulation after cocaine withdrawal (23), transporters from the nucleus accumbens and olfactory tubercle are less sensitive than those from the striatum to inhibition by nitric oxide (24), and nucleus accumbens DATs are more extensively glycosylated and are 4–5 kDa larger than striatal DATs (17, 25, 26). Because peptide mapping is a sensitive technique that can detect minor changes in amino acid sequences among closely related proteins or enzyme isoforms (27), differences in polypeptide structure between these populations of DATs might be revealed by this analysis.

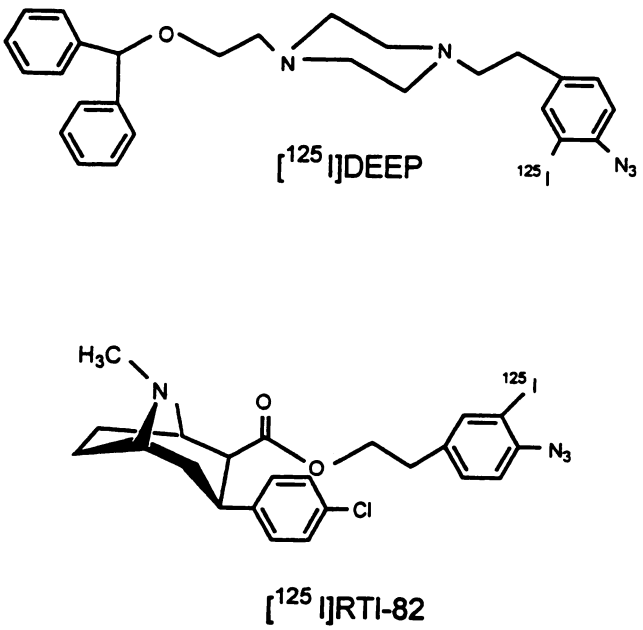

Fig. 1. Structures of [^{125}I]DEEP and [^{125}I]RTI 82.

Experimental Procedures

Preparation of photoaffinity-labeled DATs. [^{125}I]DEEP and [^{125}I]RTI 82 were synthesized by Dr. F. I. Carroll (Research Triangle Institute, Research Triangle Park, NC) and radioiodinated by Dr. John Lever (Johns Hopkins University, Baltimore, MD). Specific activity was 1000–1850 Ci/mmol. Rat striatal or nucleus accumbens membranes (20–100 mg) were homogenized in ice-cold 10 mM Na_2HPO_4 buffer, pH 7.4, containing 0.32 M sucrose, using a Brinkmann Polytron homogenizer at setting 6 for 10 sec. The homogenate was centrifuged at 20,000 × *g* for 12 min, the supernatant was discarded, and the homogenization and centrifugation were repeated. The final membrane pellet was resuspended in the same buffer at a concentration of 20 mg/ml (original wet weight). For photoaffinity labeling, membranes were diluted to 6.7 mg/ml (original wet weight) with the sucrose-phosphate buffer and radioligand was added to a final concentration of 5 nM. Binding was carried out for 1 hr at 0°, followed by irradiation of the sample with UV light for 45 sec. Membranes were washed twice by centrifugation with the same buffer, followed by solubilization with SDS-PAGE sample buffer (62.5 mM Tris, pH 6.8, 2% SDS, 10% glycerol, 10 mM dithiothreitol) at a final concentration of 20 mg/ml (original wet weight). SDS-solubilized membranes were electrophoresed on 9% acrylamide gels and DATs were identified by autoradiography. Labeled DATs were excised and electroeluted according to manufacturer's instructions (Bio-Rad), with 50–80% recovery, and were then concentrated 3–5-fold using a Centricon 30 concentrator (Amicon). The final protein concentration was 0.5–2 mg/ml.

Proteolytic digestion of DATs. Aliquots of electroeluted DAT (25 μl, 2,000–10,000 cpm) were incubated with 25 μl of *Staphylococcus aureus* V8 protease or trypsin (Boehringer Mannheim), at the indicated final enzyme concentrations, at 22° for 45 min. Enzyme solutions were prepared in 50 mM Tris·HCl, pH 8.0. At the end of the incubation, samples were either prepared directly for SDS-PAGE or 10 μl of a mixture of bovine serum albumin, ovalbumin, and soybean trypsin inhibitor (10 mg/ml each) were added to all samples, which were then subjected to immunoprecipitation. Protease-treated samples were analyzed by electrophoresis and autoradiography on 15% SDS-polyacrylamide gels. Molecular mass standards were low and high molecular mass range Rainbow markers (Amersham).

Characterization of sera and immunoprecipitation. The sera used in this study were raised against the following peptide sequences deduced from the rat DAT cDNA: peptide 15 (amino acids 6–30; CSVGPMSSVVAPAKESNAVGPREVE), peptide 16 (amino acids 42–59; LTNSTLINPPQTPVEAQE), peptide 5 (amino acids 225–236; QSRGIDDLGPPR), peptide 12 (amino acids 541–550; TFRPPHYGAY), and peptide 18 (amino acids 580–608; CSLPGSFREKLAYAITPEKDHQLVDRGEV) (see Fig. 10). For immunizations, peptides were conjugated to keyhole limpet hemocyanin, and injections and bleedings of rabbits were performed as described (20). The resulting sera, coded with the same number as the immunizing peptide, were characterized in enzyme-linked immunosorbent assays, immunoprecipitations, and immunoblots. Preimmune sera gave no positive signal above background levels, and inclusion of the specific peptide but not a nonspecific peptide blocked the immune signal.

Immunoprecipitation of DATs or DAT proteolytic fragments was performed essentially as described (20). Electroeluted DAT samples (25 μl), with or without protease treatment, were diluted 5-fold with

a buffer consisting of phosphate-buffered saline, pH 7.4, 0.05% SDS, and 0.1% Triton X-100, plus the indicated concentration of DAT antiserum. Samples were incubated for 2 hr at 4°, with gentle rotation, followed by the addition of 20 μl of Protein A-Sepharose CL-4B beads (Pharmacia) for an additional 1 hr. After the beads were washed once with the same buffer, the immune complexes were eluted from the beads with 100 μl of SDS-PAGE sample buffer and electrophoresed on 9% or 15% polyacrylamide gels. For peptide competition experiments, serum was preincubated for 15 min on ice with the indicated concentration of the immunizing peptide, an irrelevant peptide, or no peptide addition, before addition of the sample. The irrelevant peptide used against serum 16 was peptide 17 (amino acids 225–240; QSRGIDDLGPPRWQLT), and peptide 4 (amino acids 162–172; WALHYFFSSFT) was used against sera 5, 12, and 18. Immunoprecipitations were judged to be positive or negative based on comparison of preimmune and immune results and by the ability of specific peptide to block precipitation. All immunoprecipitation results shown were obtained in four to eight independent experiments.

Deglycosylation of DATs. Electroeluted DAT samples (10 μl) were adjusted to contain 0.7% Nonidet P-40 and 10 mM EDTA, in a final volume of 28 μl, and were then treated with or without 1.5 units of *N*-glycanase (Genzyme) for 18 hr at 22°, as described previously (17). Control or treated samples were then subjected to V8 proteolysis as described above and were analyzed by SDS-PAGE and autoradiography. Complete *N*-deglycosylation of transporters was verified by applying control and treated DATs to WGA-Sepharose; control transporters bound to the WGA-Sepharose and were eluted with *N*-acetylglucosamine, whereas *N*-glycanase-treated DATs failed to bind to the WGA-Sepharose.

Results

Proteolysis of DATs. When rat striatal membranes are photoaffinity labeled with either [^{125}I]DEEP or [^{125}I]RTI 82, several bands of various molecular masses are obtained. Pharmacological and immunological evidence indicates that only the 80-kDa band is the DAT (16, 18–20). For this study, the DAT band was excised from the gel and electroeluted, which produced a radiochemically pure sample, i.e., the nonspecific bands were no longer present, and all remaining radioactivity represents photolabeled DAT (see below).

The binding domains of the photoaffinity ligands were investigated by subjecting electroeluted samples to limited proteolysis with V8 protease, which cleaves at aspartic and glutamic acid residues, or trypsin, which cleaves at lysine and arginine. The resulting samples were then analyzed by electrophoresis and autoradiography. The V8 digestion patterns of [^{125}I]DEEP- and [^{125}I]RTI 82-labeled DATs are shown in Fig. 2. In the absence of V8 protease, all of the radioactivity in the sample migrated at the molecular mass of DAT and no low molecular mass forms were seen (Fig. 2, *lanes 1*, *2*, and *7*). (In these high percentage gels, DAT migrates above the 97-kDa marker. The same sample electrophoresed on a 9% gel migrates at approximately 80 kDa. See Refs. 8 and 20 for a discussion of the anomolous electrophoretic mobility of DAT.) At the lowest concentration of V8 protease, radioactivity from [^{125}I]DEEP-labeled DATs appeared in fragments migrating faster than the 14-kDa marker (Fig. 2, *lane 3*). Subsequent experiments indicated that the molecular masses of these fragments are approximately 10, 7, and 4 kDa (see Figs. 5 and 6). A slight reduction in the molecular mass of the highest molecular mass form of DAT remaining was observed, as was a 45-kDa intermediate. Increasing concentrations of V8 protease caused more radioactivity to appear in the low molecular mass forms and caused a continued reduction in size of the highest molecular mass forms remaining (Fig. 2, *lanes 4-6*). Other faint fragments between 34 and 21 kDa were also produced that were somewhat more prominent in a few experiments.

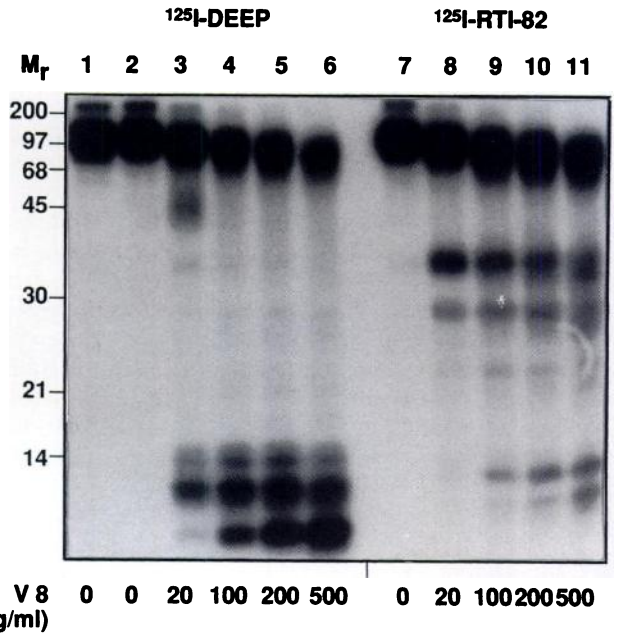

Fig. 2. V8 proteolysis of DATs. Electroeluted DATs labeled with [^{125}I]DEEP (*left*) or [^{125}I]RTI 82 (*right*) were incubated with V8 protease and then electrophoresed on a 15% polyacrylamide gel. *Lane 1*, sample was prepared directly for SDS-PAGE (no incubation); *lanes 2* and *7*, samples underwent mock incubation; *lanes 3-6* and *8–11*, samples received V8 protease as indicated. Molecular mass standards for all autoradiograms are indicated in kDa.

[^{125}I]RTI 82-labeled DATs produced a very different V8 digestion pattern. The lowest concentration of V8 protease produced two fragments, of approximately 34 and 29 kDa, and no significant fragments of lower molecular mass (Fig. 2, *lane 8*). Increasing V8 concentrations resulted in more radioactivity appearing in the 34- and 29-kDa fragments and the production of two fragments smaller than 14 kDa (Fig. 2, *lanes 9-11*). The highest molecular mass form of DAT remaining underwent incremental reduction in molecular mass with increasing V8 concentrations. In all of these experiments, higher concentrations of V8 protease and/or longer incubation times resulted in the loss of the described forms and the appearance of radioactivity that migrated at the gel dye front.

A similar analysis performed using trypsin is shown in Fig. 3. When [^{125}I]DEEP-labeled DATs were the starting material, low trypsin concentrations produced a 55-kDa fragment and minor fragments at 35, 21, 16, and 10 kDa (Fig. 3, *lane 3*). Increasing trypsin concentrations resulted in the intermediate-range fragments appearing with increasingly small molecular masses (50–40 kDa) and caused more radioactivity to appear in the smaller molecular mass forms (14 kDa and less). Tryptic digestion of [^{125}I]RTI 82-labeled DATs produced a discrete 35-kDa fragment at the lower concentrations, whereas higher concentrations produced a broad smear of radioactivity between 45 and 25 kDa and only a very small amount of radioactivity in forms of 14 kDa or less.

To verify that the proteolysis fragments were not products

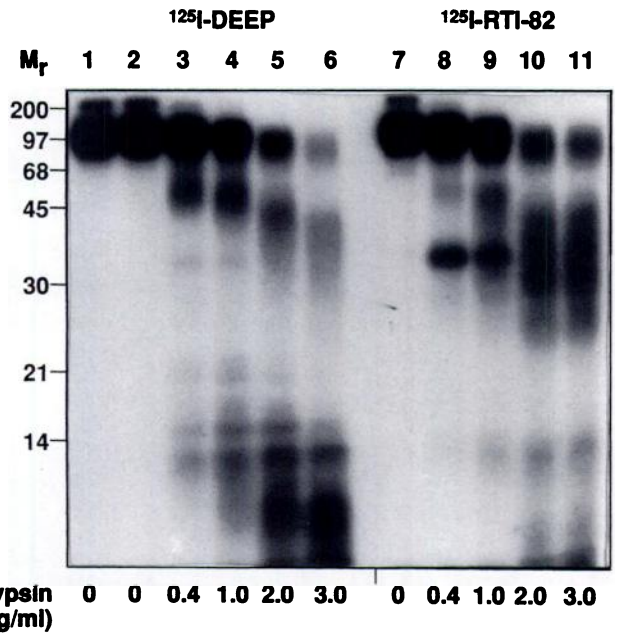

Fig. 3. Trypsin proteolysis of DATs. Electroeluted DATs labeled with [^{125}I]DEEP (*left*) or [^{125}I]RTI 82 (*right*) were incubated with trypsin and then electrophoresed on a 15% polyacrylamide gel. *Lane 1*, sample was prepared directly for SDS-PAGE (no incubation); *lanes 2* and *7*, samples underwent mock incubation; *lanes 3-6* and *8-11*, samples received trypsin as indicated.

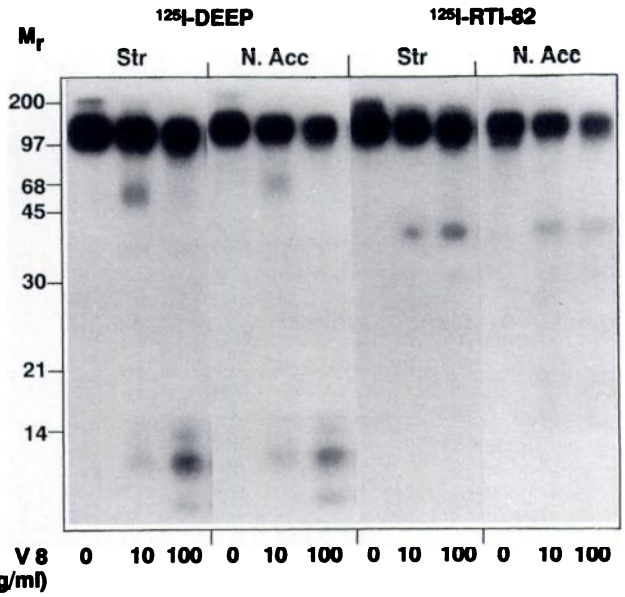

Fig. 4. Proteolysis of striatum- and nucleus accumbens-derived DATs. DATs obtained from striatum (*Str*) or nucleus accumbens (*N.Acc*) were labeled with [^{125}I]DEEP or [^{125}I]RTI 82 as indicated. The electroeluted proteins were subjected to digestion with the indicated amounts of V8 protease, followed by electrophoresis and autoradiography.

of a radioactive contaminant, control experiments were performed using membranes photolabeled in the presence of 30 μM (−)-cocaine, which blocks incorporation of the radioactive ligands. The 80-kDa region of the gel was excised, electroeluted, and analyzed with proteases in parallel with the non-cocaine-treated samples. No significant radioactivity and none of the peptide fragments described were seen using these blanked samples (data not shown), demonstrating that the proteolytic bands observed were in fact products of DAT and not of a contaminant that co-migrated in the first gel.

Comparison of striatum- and nucleus accumbens-derived DATs. To compare the polypeptide nature of DATs expressed in two different brain regions, transporters obtained from striatum and nucleus accumbens were photolabeled with [^{125}I]DEEP or [^{125}I]RTI 82 and treated in parallel with proteases. The nucleus accumbens transporters labeled with either ligand produced peptide fragment patterns indistinguishable from the striatal patterns, using either V8 protease (Fig. 4) or trypsin (data not shown). This indicates that the polypeptide characteristics of these proteins are very similar, in terms of the site of ligand incorporation, the primary sequence length between protease sites, and the presence and placement of protease sites.

Analysis of V8 fragments with antipeptide antisera. Further characterization of DAT proteolytic fragments was performed using a series of polyclonal antipeptide antibodies that recognize rat DATs in immunoprecipitation, immunoblot, and immunohistochemistry procedures (20, 28). These antibodies, which are directed against the amino and carboxyl termini and two intervening regions (see Fig. 10) were used in immunoprecipitation assays to analyze the DAT proteolytic fragments. Because of their more discrete appearence, compared with the tryptic fragments, the V8 preparations were used for most of the immunoprecipitation experiments. Positive and negative controls were provided by precipitation of unproteolyzed transporters and precipitation of V8 digests with the corresponding preimmune sera, respectively. The sera exhibited different potencies against DAT, with the following rank order: 16 ⩾ 5 > 15 = 12 = 18; sera 16 and 5 were used at lower dilutions than the others. When each immune serum was compared with its matching preimmune serum, concentrations were identical; however, regardless of dilution, all preimmune sera produced comparable signals of negligible intensity.

The interpretation of the immunoprecipitation experiments is that lack of precipitability indicates that the epitope is not present on the fragment. Although an alternative interpretation could be that lack of precipitation results from a ligand-induced conformational change in the fragment, resulting in loss of immune recognition, this seems unlikely, because all sera precipitated unproteolyzed transporters with incorporated ligand. However, immunoanalysis of fragments generated from metabolically labeled transporters could be used to investigate this possibility.

When V8 fragments from [^{125}I]DEEP-labeled transporters were screened with this series of antibodies, the 10- and 7-kDa fragments were immunoprecipitated by serum 16 (Figs. 5 and 6). The 4-kDa fragment was not recognized, and none of these low molecular mass fragments was precipitated by any of the other sera. The 45-kDa intermediate was recognized by sera 15, 16, and 5. The highest molecular mass band was precipitated by all sera, although its recognition by sera 15 and 18 was reduced, compared with unproteolyzed controls, indicating that an end-inward proteolysis causes the incremental molecular mass reduction of this form. None of the fragments was recognized by preimmune serum (Fig. 5, *lane 7*) (all preimmune sera were tested and gave comparable results). Precipitation of the 10- and 7-kDa V8 fragments by serum 16 was specific, because precipitation was blocked by inclusion of peptide 16, but not a nonspecific

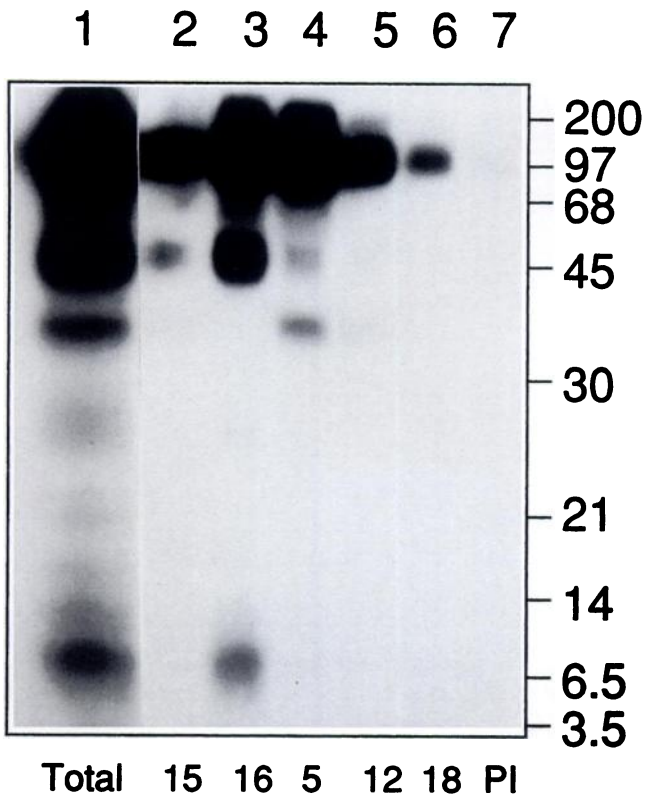

Fig. 5. Immunoprecipitation of V8 digest of [^{125}I]DEEP-labeled DATs. Electroeluted photolabeled DATs were treated with V8 protease (0.1 mg/ml) and immunoprecipitated with the indicated antipeptide antisera diluted as follows: serum 15, 1/30; serum 16, 1/100; serum 5, 1/40; serum 12, 1/30; serum 18, 1/30; preimmune serum 16 (*PI*), 1/100. *Lane 1*, input sample. The immunopellets were electrophoresed on 15% polyacrylamide gels and the resulting autoradiogram is shown.

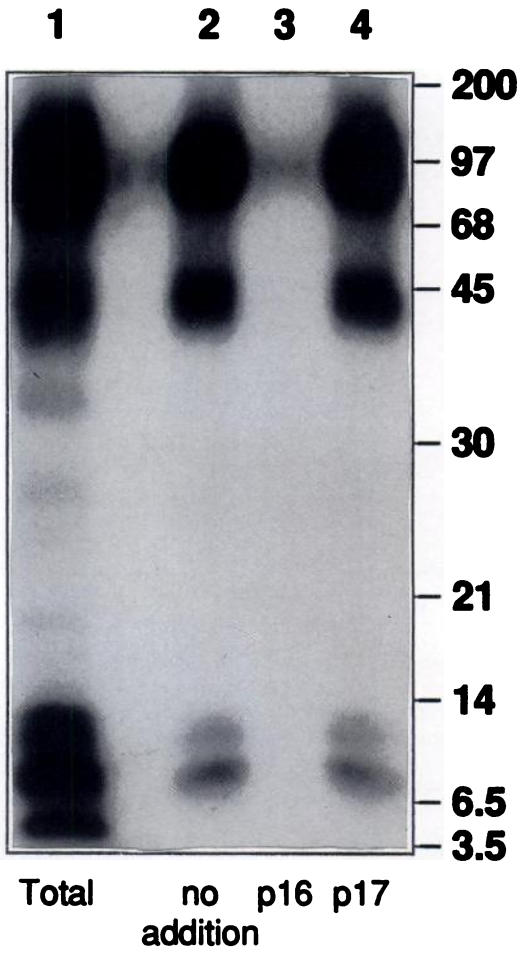

Fig. 6. Prevention of immunoprecipitation with specific peptide. [^{125}I]DEEP-labeled DATs were treated with 0.1 mg/ml V8 protease and immunoprecipitated with serum 16 diluted 1/200, which received either no peptide preincubation (*lane 2*), preincubation with 20 μg/ml peptide 16 (*lane 3*), or preincubation with 20 μg/ml peptide 17 (*lane 4*). *Lane 1*, input sample.

peptide, in the immunoprecipitation assay (Fig. 6). These results have been produced in six independent experiments. In two of these, including the one shown in Fig. 5, there was a greater than usual production of the 34-kDa fragment (compare with [^{125}I]DEEP-labeled V8 digests in Figs. 2, 4, and 9). This band was precipitated with serum 5 (Fig. 5, *lane 4*) but was not characterized more fully because of the irreproducibility of its production.

The 34-kDa [^{125}I]RTI 82-labeled V8 fragment was recognized robustly by serum 5 and less strongly, but above preimmune levels, by sera 12 and 18 (Fig. 7). Precipitation of this fragment with these three sera was blocked by inclusion of the specific peptide, but not a nonspecific peptide, during the procedure (Fig. 8). A small amount of this fragment was present in the immunopellet of serum 15 in Fig. 7, but this was nonspecific, because it did not appear in all experiments and was not blocked by peptide during immunoprecipitation. The 35-kDa [^{125}I]RTI 82-labeled tryptic fragment described in Fig. 3 was also analyzed with these antibodies and was also precipitated by sera 5, 12, and 18, but not by sera 15 or 16 (data not shown), indicating that similarly sized fragments with the same immunological characteristics are generated by V8 protease and trypsin. The 29-kDa [^{125}I]RTI 82-labeled V8 fragment could not be characterized, due to its low abundance.

Carbohydrate analysis of V8 fragments. As an additional method to substantiate the location of these photolabeled domains, enzymatic deglycosylation of DATs was combined with proteolysis to determine whether *N*-linked carbohydrates were present on the V8 fragments. Treatment of DATs with *N*-glycanase removes asparagine-linked carbohydrates, which is manifested as a reduction in apparent molecular mass (26, 29). As shown in Fig. 9, *N*-glycanase treatment of DAT resulted in a change in electrophoretic mobility from 80 kDa (Fig. 9, *lanes 1* and *5*) to approximately 50 kDa (Fig. 9, *lanes 2* and *6*). V8 proteolysis of undeglycosylated DATs produced the characteristic 45-, 10-, 7-, and 4-kDa fragments from [^{125}I]DEEP-labeled DATs (Fig. 9, *lane 3*) and the 34- and 29-kDa fragments from [^{125}I]RTI 82-labeled DATs (Fig. 9, *lane 7*). Fig. 9, *lanes 4* and *8*, shows transporters that were first deglycosylated and then treated with V8 protease. The proteolysis patterns of these samples were identical to those derived from control DATs, except for the appearance of a doublet at about 24 kDa in the [^{125}I]DEEP-labeled sample. This was probably the deglycosylated form of the 45-kDa fragment seen in Fig. 9, *lane 3*, which was precipitated by sera raised to peptides that flank the region containing the consensus glycosylation sites (sera 15, 16, and 5) (Fig. 5). The molecular masses of the 10-, 7-, and 4-kDa [^{125}I]DEEP-labeled fragments and the 34- and 29-kDa [^{125}I]RTI 82-labeled fragments were unaffected by

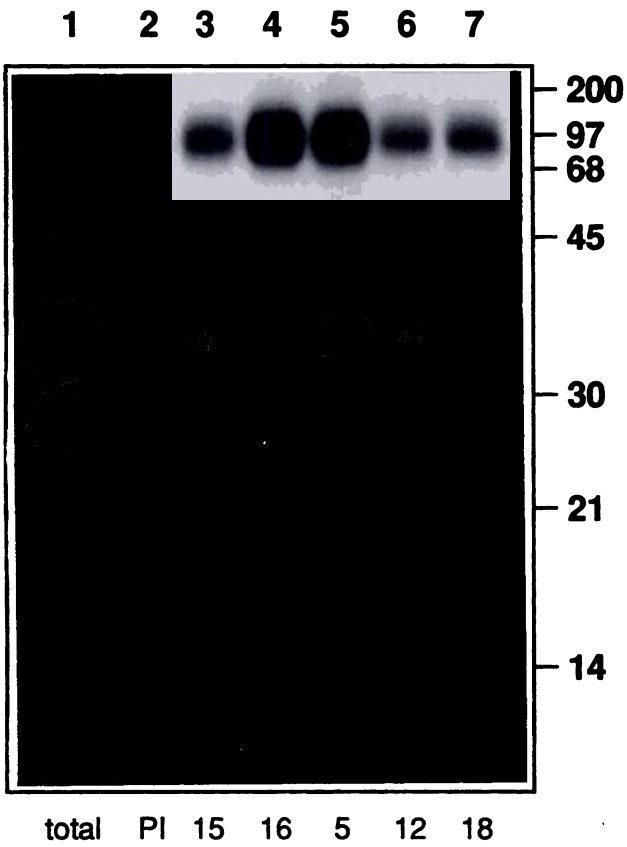

Fig. 7. Immunoprecipitation of V8 digest of [^{125}I]RTI 82-labeled DATs. Electroeluted DATs were treated with 0.3 mg/ml V8 protease and immunoprecipitated with the indicated antipeptide sera diluted as follows: serum 15, 1/30; serum 16, 1/100; serum 5, 1/40; serum 12, 1/30; serum 18, 1/30; preimmune serum 5 (*PI*), 1/40. *Lane 1*, input sample.

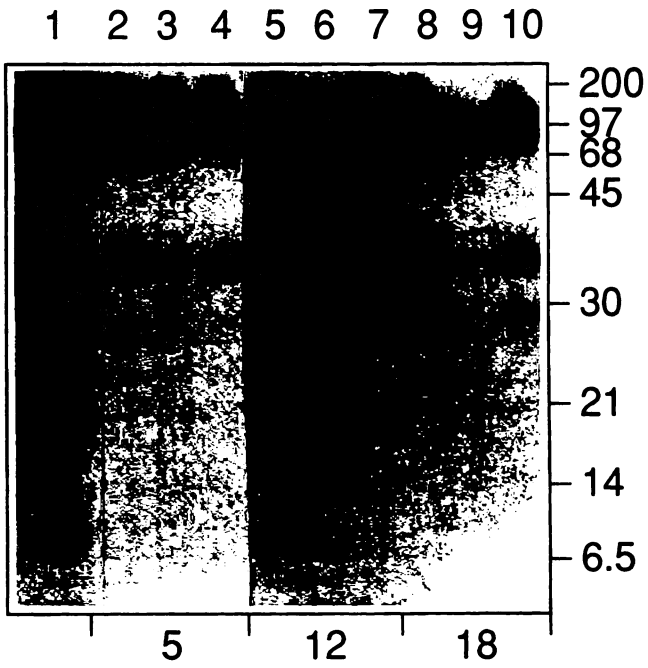

Fig. 8. Prevention of immunoprecipitation with specific peptide. [^{125}I]RTI 82-labeled DATs treated with 0.3 mg/ml V8 protease were immunoprecipitated with sera 5, 12, and 18, as indicated, at the same dilutions as shown in Fig. 7. Each serum received preincubation either without peptide (*lanes 2*, *5*, and *8*), with the immunizing peptide (50 μg/ml) (*lanes 3*, *6*, and *9*), or with an irrelevant peptide (peptide 4, 50 μg/ml) (*lanes 4*, *7*, and *10*). *Lane 1*, input sample.

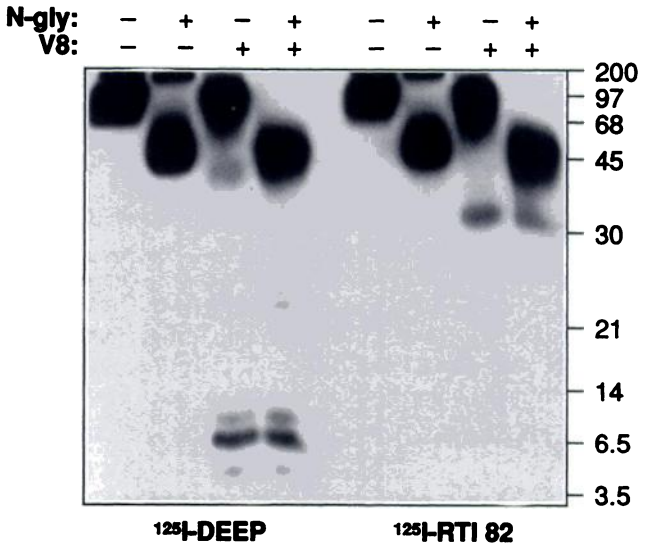

Fig. 9. Co-treatment of DATs with *N*-glycanase (*N-gly*) and V8 protease. Electroeluted DATs labeled with [^{125}I]DEEP (*left*) or [^{125}I]RTI 82 (*right*) were treated first with *N*-glycanase or incubation buffer only, followed by V8 (0.1 mg/ml) proteolysis. The samples were electrophoresed on 15% polyacrylamide gels and the resulting autoradiogram is shown. *Symbols at the top*, enzyme combinations used. Lanes are numbered 1–8, left to right.

deglycosylation (Fig. 9, *lanes 3*, *4*, *7*, and *8*). The higher molecular mass V8 fragments (those above 50 kDa) remained sensitive to *N*-glycanase, and the molecular mass losses due to *N*-glycanase or V8 treatment were additive in the combination treatment. Reversal of the order of enzyme treatment, i.e., V8 proteolysis first, followed by *N*-glycanase treatment, produced the same result, demonstrating that the proteolytic fragments do not contain glycosylation sites that are inaccessible to *N*-glycanase before proteolysis.

Discussion

This study analyzes the binding sites on DATs for [^{125}I]DEEP and [^{125}I]RTI 82, ligands that represent two classes of compounds, i.e., GBR compounds and cocaine, that have been used extensively to characterize DATs. This is the first identification of a cocaine-binding region on a neurotransmitter transporter using a positive function approach (as opposed to a mutagenesis loss-of-function approach) and is the first analysis of any kind regarding localization of the GBR binding site.

Proteolysis of [^{125}I]DEEP- and [^{125}I]RTI 82-labeled DATs with V8 protease or trypsin produced highly reproducible patterns of low and medium molecular mass fragments containing the incorporated photolabel, and the peptide fragment patterns produced were different for each enzyme. This technique was used to compare the polypeptide structures of transporters expressed in the striatum and nucleus accumbens, brain regions containing dopaminergic synaptic terminals originating from different cell body groups. All combinations of enzymes and ligands yielded identical peptide maps, indicating that these proteins are, at least, highly similar in primary sequence and suggesting that the differential regulation of these proteins by cocaine and nitric oxide is the result of differences in post-translational events or

enzymatic differences between cell types. Although DATs from nucleus accumbens and striatum have undergone numerous functional comparisons, this study represents the first comparison of these transporters at the polypeptide level and supports the contention that these transporters are derived from a single gene.

Proteolysis of DAT was also investigated using other enzymes, including endoproteinase Arg-C, endoproteinase Lys-C, and endoproteinase Asp-N, which cleave specifically at the indicated residues, and it was found in all cases that the peptide patterns were different for [^{125}I]DEEP- and [^{125}I]RTI 82-labeled DATs (data not shown). The production of different peptide patterns, particularly with several different enzymes, suggests that the radioactive ligands are incorporated into different sites on the polypeptide, supporting the hypothesis that these compounds interact by an apparently noncompetitive mechanism, as has been suggested by many ligand binding studies (11–14). An alternative explanation of these results is that ligand binding to the protein produces a conformational change that results in altered proteolytic cleavage patterns, a phenomenon that has been observed with numerous proteins, including the closely related γ-aminobutyric acid transporter (30). Because of this uncertainty in interpretation, the photolabeled fragments were analyzed further by immunoprecipitation with epitope-specific antisera. This enabled the domains containing the ligands to be localized to specific regions of the protein and verified that the ligands were differentially incorporated into the polypeptide.

The 10- and 7-kDa [^{125}I]DEEP-labeled V8 fragments were immunoprecipitated with anti-peptide 16 antiserum, and this precipitation was blocked by the homologous peptide but not a heterologous peptide. The 4-kDa fragment was not precipitated by serum 16, indicating that, if it is a product of the 10- or 7-kDa fragment, the cleavage that results in the loss of molecular mass includes the region of epitope 16. None of the other sera precipitated these fragments, and the fragments were not changed in apparent molecular mass by pretreatment of DATs with *N*-glycanase. These results (shown schematically in Fig. 10) indicate that [^{125}I]DEEP is incorporated into the DAT in a region that includes the epitope of peptide 16, just before TMD 1, and extends carboxyl-terminally but ends before reaching a utilized glycosylation site on the putative large extracellular loop. Because serum 15 does not recognize the low molecular mass DAT fragments, the extreme amino terminus of the protein, containing that epitope, is probably proteolyzed, but the exact amino terminis of these fragments cannot be ascertained from these data. There are four glutamic acid residues that could serve as cleavage sites resulting in the loss of epitope 15 but not epitope 16 (amino acids 20, 28, 30, and 36). The apparent molecular masses of the 10- and 7-kDa fragments indicate that they extend carboxyl-terminally approximately 90 and 64 amino acids, respectively, placing the carboxyl termini in the vicinity of TMDs 2 and 3. Glutamic acid residues, which could serve as the carboxyl-terminal cleavage sites in this scenario, are present at positions 79, 117, and 126, depending on the amino-terminal cleavage site. The 4-kDa fragment could lose serum 16 immunoreactivity due to cleavage of one of the three glutamic acids at the carboxyl-terminal end of sequence 16 (amino acid 56, 59, or 61) or slightly more carboxyl-terminal aspartic acids (amino acid 68 or 79). In a minority of experiments a small amount of [^{125}I]DEEP became incorporated into a 34-kDa fragment immunoprecipitated by serum 5 but not by serum 16, indicating that under some conditions a small fraction of [^{125}I]DEEP becomes incorporated into what is probably the same domain as that of [^{125}I]RTI 82 (see below).

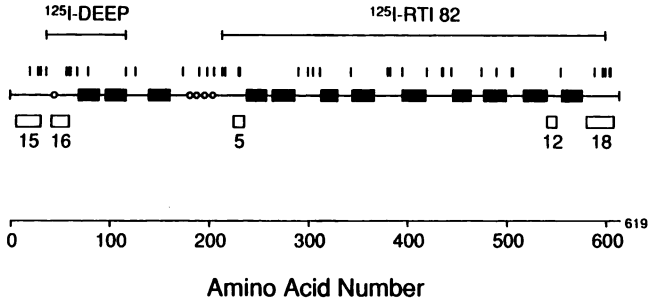

Fig. 10. Diagram of DAT showing putative TMDs (*closed rectangles*), location of immunizing peptides (*open rectangles*), consensus *N*-glycosylation sites (*circles*), and aspartic and glutamic acid residues (*tick marks*). *Lines above the primary sequence*, location of the 10-kDa [^{125}I]DEEP-labeled and 34-kDa [^{125}I]RTI 82-labeled fragments described in the text. The amino and carboxyl termini shown for these regions are consistent with the data presented but are to a certain degree arbitrary and are not meant to signify the positions of the termini with absolute certainty.

It should be kept in mind that that the model presented here is based on the apparent molecular masses of the peptide fragments, which may, like the intact DAT, migrate with anomolously high electrophoretic mobility, and definitive identification of the amino and carboxyl termini of the fragments will require purification and amino acid sequencing. In addition, because it is not possible to predict which amino acid residues willl form the covalent attachment to the azido group of the ligand, purification and sequencing will also be required for identification of the ligand attachment site.

The 34-kDa [^{125}I]RTI 82-labeled fragment produced by V8 protease treatment was precipitated with sera 5, 12 and 18, placing it carboxyl-terminally to the [^{125}I]DEEP-labeled fragments. Because the molecular mass of this fragment was not affected by *N*-glycanase treatment, it also does not contain any utilized glycosylation sites, and thus the amino terminus of this fragment lies between the glycosylation sites and sequence 5. Because it is not known which of the consensus glycosylation sites are utilized, it is not possible to determine which V8 cleavage site represents the amino terminus of this fragment. The carboxyl terminus of this fragment is defined by serum 18 immunoreactivity, although it does not necessarily extend to the end of sequence 18, because there may be many immunoreactive epitopes in this long (28-amino acid) sequence. The apparent molecular mass of this fragment is somewhat low for it to be encompassed by these three epitopes, which at a minimum (assuming the serum 18-immunoreactive epitope to be close to TMD 12) include 360 amino acids, thus yielding an estimated molecular mass of about 40 kDa. The reason for this size discrepancy is not known, although, again, it may be a reflection of the overall anomolously high electrophoretic mobility of DAT on SDS gels. However, immunoprecipitation of this fragment with the three sera appears to be specific, because in all cases precipitation is blocked by the homologous peptide but not a heterologous peptide. Potential V8 cleavage sites are present in appropriate places of the primary sequence to produce the

fragments shown, i.e., between the consensus glycosylation sites and the beginning of epitope 5 (amino acids 191, 199, 205, 214, and 217) and in the carboxyl-terminal regions of epitope 18 (amino acids 588, 597, 599, 604, and 607).

This study also provides experimental evidence that *N*-glycosylation of the transporter does occur in the region between TMDs 3 and 4. Because the *N*-linked carbohydrates are not present on the 10- or 7-kDa [^{125}I]DEEP-labeled fragments or on the 34- or 29-kDa [^{125}I]RTI 82-labeled fragments, the only remaining regions available to contain the carbohydrates are the region between these two domains and the extreme amino and carboxyl termini. The carboxyl terminus contains no consensus *N*-glycosylation sequences and, although there is a canonical glycosylation site in the amino-terminal domain (amino acid 44), it is present within the sequence of peptide 16. Because the 10- and 7-kDa [^{125}I]DEEP-labeled fragments are precipitated by serum 16 but are not changed in molecular mass by *N*-glycanase treatment, it is unlikely that this site is used. Thus, after elimination of the photolabeled domains as possessing the carbohydrates, the only remaining region of the polypeptide capable of possessing *N*-linked carbohydrates is that between TMDs 3 and 4. These findings also provide some support for the presently accepted topological model of the DAT, i.e., with the initial hydrophilic amino stretch presumably being oriented cytoplasmically and the hydrophilic sequence between putative TMDs 3 and 4 being oriented extracellularly.

These mapping results are thus internally consistent with regard to all physical landmarks involved, i.e., the positions of the epitopes, the consensus glycosylation sites, and potential V8 cleavage sites. These results can also be interpreted as being consistent with some of the DAT structure-function relationships determined recently using molecular approaches. For example, the amino-terminal region of DAT has been found to be critical for uptake, being implicated by chimeric approaches as being important either for DA affinity (TMDs 1–3) (31) or for generalized translocation mechanisms (TMDs 1–5) (32). This region is also highlighted by site-directed mutagenesis, because Asp-79 in TMD 1 is essential for DA uptake (33). The finding that [^{125}I]DEEP labels this precise region suggests that GBR compounds inhibit DA uptake by interfering with an essential transport function provided by this domain. With regard to cocaine binding, Giros *et al.* (32) reported reduced cocaine inhibition of transport by DAT-norepinephrine transporter chimeras with junctions in TMDs 5–8, and mutation of Tyr-250 in TMD 4 substantially reduced (−)-2β-[^{3}H]carbomethoxy-3β-(4-fluorophenyl)tropane binding without affecting DA uptake (34), findings that correlate well with the peptide map results showing [^{125}I]RTI 82 incorporation in the region delineated by TMDs 4–12.

However, it should also be noted that there are probably numerous determinants for binding scattered throughout the primary polypeptide sequence and that the peptide fragments identified with photoaffinity ligands may possess only one or some of these determinants. This could explain, for instance, the finding that the Asp-79 mutation in TMD 1 reduces (−)-2β-[^{3}H]carbomethoxy-3β-(4-fluorophenyl)tropane binding as well as DA uptake (30) but this region of the DAT protein is not labeled by [^{125}I]RTI 82. It is also possible that the residues that are important for binding of ligands are not the residues to which the photoreactive groups become attached, such that photolabel incorporation occurs at residues that are close to the binding pocket three-dimensionally but distant in primary sequence. However, in the absence of additional data this scenario should not be presumed to be true, and incorporation of these ligands may occur near one of the binding determinants. The convergence of evidence from this study with that of the molecular approaches suggests that this may, in fact, be the case. Clarification of these issues will require further identification of functional determinants, elucidation of structural topology, and, ultimately, crystallographic determination of DAT three-dimensional structure.

Acknowledgments

The author expresses sincere appreciation to Dr. Michael J. Kuhar for providing the supportive work environment that led to this study and to Mr. Michael McCoy for his outstanding technical assistance. Valuable comments were offered by Drs. Chris Surrat, Steven Davis, Amy Newman, and Ivy Carroll.

References

1. Horn, A. S. Dopamine uptake: a review of progress in the last decade. *Prog. Neurobiol.* **34**:387–400 (1990).
2. Giros, B., S. El Mestikawy, N. Godinot, K. Zheng, H. Han, T. Yang-Feng, and M. G. Caron. Cloning, pharmacological characterization, and chromosome assignment of the human dopamine transporter. *Mol. Pharmacol.* **42**:383–390 (1992).
3. Vandenbergh, D. J., A. M. Persico, and G. R. Uhl. A human dopamine transporter cDNA predicts reduced glycosylation, displays a novel repetitive element, and provides racially-dimorphic *Taq*I RFLPs. *Mol. Brain Res.* **15**:161–166 (1992).
4. Kilty, J. E., D. Lorang, and S. G. Amara. Cloning and expression of a cocaine-sensitive rat dopamine transporter. *Science (Washington D. C.)* **254**:578–579 (1991).
5. Shimada, S., S. Kitayama, C.-L. Lin, A. Patel, E. Nanthakumar, P. Gregor, M. Kuhar, and G. Uhl. Cloning and expression of a cocaine-sensitive dopamine transporter complementary DNA. *Science (Washington D. C.)* **254**:576–578 (1991).
6. Usdin, T. B., E. Mezey, C. Chen, M. J. Brownstein, and B. J. Hoffman. Cloning of the cocaine-sensitive bovine dopamine transporter. *Proc. Natl. Acad. Sci. USA* **88**:11168–11171 (1991).
7. Carroll, F. I., A. H. Lewin, J. W. Boja, and M. J. Kuhar. Cocaine receptor: biochemical characterization and structure-activity relationships of cocaine analogues at the dopamine transporter. *J. Med. Chem.* **35**:969–981 (1992).
8. Boja, J. W., R. A. Vaughan, A. Patel, E. Shaya, and M. J. Kuhar. The dopamine transporter, in *Dopamine Receptors and Transporters: Pharmacology, Structure, and Function* (H. B. Niznik, ed.). Marcel Dekker, New York, 611–644 (1994).
9. Reith, M. A., B. de Costa, K. C. Rice, and A. E. Jacobsen. Evidence for mutually exclusive binding of cocaine, BTCP, GBR 12935, and dopamine to the dopamine transporter. *Eur. J. Pharmacol.* **227**:417–425 (1992).
10. Meiergerd, S. M., and J. O. Schenk. Kinetic evaluation of the commonality betwen the site(s) of action of cocaine and some other structurally similar and dissimilar inhibitors of the striatal transporter for dopamine. *J. Neurochem.* **63**:1683–1692 (1994).
11. Madras, B. K., R. D. Spealman, M. A. Fahey, J. L. Neumeyer, J. K. Saha, and R. A. Milius. Cocaine receptors labeled by [^{3}H]2β-carbomethoxy-3β-(4-fluorophenyl)tropane. *Mol. Pharmacol.* **36**:518–524 (1989).
12. Berger, P., J. P. Elsworth, M. E. A. Reith, D. Tanen, and R. H. Roth. Complex interaction of cocaine with the dopamine uptake carrier. *Eur. J. Pharmacol.* **176**:251–252 (1990).
13. Maurice, T., G. Barbanel, J.-M. Kamenka, and J. Vignon. Endogenous dopamine differently afffects *N*-[1-(2-benzo(*b*)thiophenyl)cyclohexyl]-piperidine ([^{3}H]BTCP, a phencyclidine derivative) binding to the dopamine uptake complex. *Neuropharmacology* **30**:591–598 (1991).
14. Pristupa, Z. B., J. M. Wilson, B. J. Hoffman, S. J. Kish, and H. B. Niznik. Pharmacological heterogeneity of the cloned and native human dopamine transporter: disassociation of [^{3}H]WIN 35,428 and [^{3}H]GBR 12,935 binding. *Mol. Pharmacol.* **45**:125–135 (1994).
15. Uhl, G. Neurotransmitter transporters (plus): a promising new gene family. *Trends Neurosci.* **15**:265–268 (1992).
16. Grigoriadis, D. E., A. A. Wilson, R. Lew, J. S. Sharkey, and M. J. Kuhar. Dopamine transport sites selectively labeled by a novel photoaffinity probe: [^{125}I]DEEP. *J. Neurosci.* **9**:2664–2670 (1989).
17. Lew, R., A. Patel, R. A. Vaughan, A. Wilson, and M. J. Kuhar. Microhet-

erogeneity of dopamine transporters in rat striatum and nucleus accumbens. *Brain Res.* **584:**266–271 (1992).
18. Patel, A., J. W. Boja, J. Lever, R. Lew, R. Simantov, F. I. Carroll, A. H. Lewin, A. Philip, Y. Gao, and M. J. Kuhar. A cocaine analog and a GBR analog label the same protein in rat striatal membranes. *Brain Res.* **576:**173–174 (1992).
19. Patel, A., G. Uhl, and M. J. Kuhar. Species differences in dopamine transporters: postmortem changes and glycosylation differences. *J. Neurochem.* **61:**496–500 (1993).
20. Vaughan, R. A., G. Uhl, and M. J. Kuhar. Recognition of dopamine transporters by antipeptide antibodies. *Mol. Cell. Neurosci.* **4:**209–215 (1993).
21. Bjorklund, A., and O. Lindvall. Dopamine-containing systems in the CNS, in *A Handbook of Chemical Neuroanatomy, Vol. 2, Classical Transmitters in the CNS* (A. Bjorklund and T. Hokfelt, eds.). Elsevier, New York, 55–122 (1984).
22. Ritz, M. C., R. J. Lamb, S. R. Goldberg, and M. J. Kuhar. Cocaine receptors on dopamine transporters are related to self-administration of cocaine. *Science (Washington D. C.)* **237:**1219–1223 (1987).
23. Pilotte, N. S., L. G. Sharpe, and M. J. Kuhar. Withdrawal of repeated intravenous infusions of cocaine persistently reduces binding to dopamine transporters in the nucleus accumbens of Lewis rats. *J. Pharmacol. Exp. Ther.* **269:**963–975 (1994).
24. Pogun, S., M. H. Baumann, and M. J. Kuhar. Nitric oxide inhibits [^{3}H]-dopamine uptake. *Brain Res.* **641:**83–91 (1994).
25. Lew, R., R. Vaughan, R. Simantov, A. Wilson, and M. J. Kuhar. Dopamine transporters in the nucleus accumbens and the striatum have different apparent molecular weights. *Synapse* **8:**152–153 (1991).
26. Lew, R., D. Grigoriadis, A. Wilson, J. W. Boja, R. Simantov, and M. J. Kuhar. Dopamine transporter: deglycosylation with exo- and endoglycosidases. *Brain Res.* **539:**239–246 (1991).
27. Cleveland, D. W., S. G. Fischer, M. W. Kirschner, and U. Laemmli. Peptide maping by limited proteolysis in sodium dodecyl sulfate and analysis by gel electrophoresis. *J. Biol. Chem.* **252:**1102–1106 (1977).
28. Grant, S., R. Revay, R. Vaughan, C. Freed, G. Uhl, and M. J. Kuhar. Immunohistochemical localization of dopamine transporters in rat brain. *Soc. Neurosci. Abstr.* **20:**920 (1994).
29. Sallee, F. R., E. L. Fogel, E. Schwartz, S.-M. Choi, D. P. Curran, and H. B. Niznick. Photoaffinity labeling of the mammalian dopamine transporter. *FEBS Lett.* **256:**219–224 (1989).
30. Mabjeesh, N. J., and B. I. Kanner. The substrates of a sodium- and chloride-coupled γ-aminobutyric acid transporter protect multiple sites throughout the protein against proteolytic cleavage. *Biochemistry* **32:** 8540–8546 (1993).
31. Buck, K. J., and S. G. Amara. Chimeric dopamine-norepinephrine transporters delineate structural domains influencing selectivity for catecholamines and 1-methyl-4-phenylpyridinium. *Proc. Natl. Acad. Sci. USA* **91:**12584–12588 (1995).
32. Giros, B., Y.-M. Wang, S. Suter, S. B. McLeskey, C. Pifl, and M. G. Caron. Delineation of discrete domains for substrate, cocaine, and tricyclic antidepressant interactions using chimeric dopamine-norepinephrine transporters. *J. Biol. Chem.* **269:**15985–15988 (1994).
33. Kitayama, S., S. Shimada, H. Xu, L. Markham, D. M. Donovan, and G. R. Uhl. Dopamine transporter site-directed mutations differentially alter substrate transport and cocaine binding. *Proc. Natl. Acad. Sci. USA* **89:** 7782–7785 (1992).
34. Wang, J. B., S. Davis, and G. Uhl. Dopamine transporter site-directed mutants identify residues selectively important for cocaine recognition. *Soc. Neurosci. Abstr.* **19:**745 (1993).

Send reprint requests to: Roxanne A. Vaughan, NIDA Addiction Research Center, 4940 Eastern Ave., Baltimore, MD 21224.